Sensors for Automatic Process Control of Wire Bonding

S.W. Or[1,2], H.L.W. Chan[1], V.C. Lo[1] and C.W. Yuen[2]
[1]Department of Applied Physics and Materials Research Center
The Hong Kong Polytechnic University, Hunghom, Kowloon, Hong Kong
[2]ASM Assembly Automation Ltd.
4/F, Watson Center, 16 Kung Yip Street, Kwai Chung, Hong Kong

Abstract — PZT sensors were installed on an ultrasonic transducer used for wire bonding in order to record ultrasonic amplitude and bonding time during the bonding process. To find an appropriate location for the sensor placement, the vibration displacement distributions of the transducer were measured using a high frequency heterodyne interferometer. The non-linear signal detected by the PZT sensor was processed and the signatures of the higher frequency harmonics were recorded and related to the bonding quality. The change in harmonic contents and its relation with bond quality will be used to develop a real-time automatic process control system for wire bonding.

I. INTRODUCTION

In microelectronic packaging, wire bonding provides electrical interconnections between chips and their associated circuitry. Historically, it has been recognized that the wire bonding process can be liable to significant variations in bond quality and that wire bonds are not amenable to conventional NDT weld inspection techniques. Current bond quality assurance / control techniques mainly consist of periodic calibration of the bonding machine for uniform bond quality, visual inspection of the degree of wire deformation and batch destructive testing after bonding. This is clearly an expensive and time consuming process. There is difficulty in the attainment of cost effective quality assurance standards [1], for which the requirement is increasing in importance as a result both of the growing use of wire bonded circuits and of the increasing adoption of automatic bonding machines capable of high production rates with only limited supervision. Therefore, in-process monitoring and control of wire bonding process is required.

In this paper, we demonstrate how to use piezoelectric sensors in automatic process control of wire bonding by observing the change in high order harmonics of the ultrasonic signal.

II. VIBRATION DISPLACEMENT DISTRIBUTIONS MEASUREMENT USING LASER INTERFEROMETRY

A. Principle of Detection

A Mach-Zehnder type heterodyne interferometer (SH-120 from B. M. industries in France) was used to measure the ultrasonic displacements of an ultrasonic transducer (Fig. 1) [2]. A horizontally polarized laser beam (frequency f_L; wave number $k = 2\pi/\lambda$, $\lambda = 6328$ Å for He-Ne laser) is splitted into a reference beam R and a probe beam P. The reference beam is directed through a dove prism into a photodiode. The frequency of the probe beam is first shifted by f_B (70 MHz) in a Bragg cell, and the reflected beam S is then phase modulated by the ultrasonic displacement of the transducer $\phi(t)$. For a sinusoidal displacement of the surface $\phi(t) = u[\sin(\omega_o t)]$, where u and ω_o are ultrasonic displacement and frequency of the transducer respectively, the interference of two beams on the photodetector delivers a beat signal proportional to $\cos[\omega_B t+(2ku)\sin(\omega_o t)]$. The frequency spectrum of this signal contains sidebands at frequencies $\omega_B \pm n\omega_o$, where n = 1, 2, 3, ... Each sideband has a relative amplitude equal to the Bessel function $J_n(x)$, where $x = 4\pi u/\lambda$. The ratio R_n between the carrier level $J_0(x)$ and the sideband levels $J_n(x)$ provides an absolute amplitude of the ultrasonic displacement. That is,

$$R_n = 10^{R_n'/20} = J_n(x)/J_0(x) \qquad n = 1,2,...$$

The value of R_n' in dBm can be read from a spectrum analyzer (HP 3589A). Then, R_n in linear scale is obtained and hence the unknown x. The ultrasonic displacement is

$$u = x\lambda/4\pi$$

The photon noise limits the detectivity to 10^{-4} Å, for a 1 Hz detection bandwidth [3]. For a 45 MHz bandwidth, the minimum detectable displacement is about 0.7 Å. From Bessel function of the 1st kind, at $x \approx 2.4$, $J_0(x)$ will be zero [4]. Thus, x is limited to this value in practice. For small displacements, i.e. u < 100 Å, only the components at f_B and $f_B \pm f_o$ are significant [2].

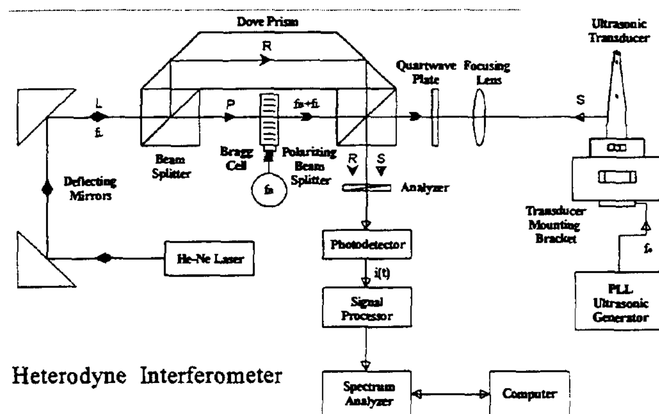

Fig. 1. Experimental setup.

0-7803-3355-1/96/$5.00 © 1996 IEEE.

Authorized licensed use limited to: Hong Kong Polytechnic University. Downloaded on December 1, 2008 at 20:40 from IEEE Xplore. Restrictions apply.

B. Displacement Distributions of the Concentrator

Experimentally, the transducer was mounted on a micromanipulator with movements in the x, y, z, and θ directions and clamped as it would be in a wire bonder. The orientation of the transducer was adjusted carefully so that the laser beam was normal to the vibration surface and maximum signal level on the spectrum analyzer was obtained. The driving voltage was 3.7 $V_{p\text{-}p}$ at the transducer terminal to initiate optimum bonding condition. The vibration displacement distributions of the concentrator (coupler and exponential horn) at 62.5 kHz were measured, in steps of 0.5 mm, along the dotted lines 'a' (top scanning), 'b' (bottom scanning), 'c' (LHS scanning), and 'd' (RHS scanning), while the laser beam impinges on the transducer along directions 'A', 'B', 'C', and 'D' respectively (Fig. 2). The results are shown in Fig. 3. The error of this experiment by comparing the results of $J_1(x)/J_0(x)$ to those of $J_2(x)/J_0(x)$ (not shown) is about 10%, and the measurements are typically reproducible to within about 20%.

The distributions agreed well for the LHS and RHS scannings. The displacement nodes and antinodes are located at similar locations on the concentrator. However, those for the top and bottom scannings are not well matched. The displacement nodes and antinodes are 180° out of phase in the first 20 mm (coupler), and at more or less the same locations in the last 40 mm section (horn). The mismatch in the first 20 mm may be due to asymmetric clamping (3-points clamping) and lack of geometric symmetry of the transducer. The degree of similarity increases with length in order to satisfy the common boundary conditions at the end of the horn. The vibration displacements are amplified by the exponential horn, and at about 59.75 mm where the wedge is clamped, the displacements are small but non-zero.

Displacement patterns for the top and bottom scannings are different from those for side scannings. Pure coaxial radial mode displacement caused by longitudinal stress distribution was not observed in practical system [5, 6]. In order to control the vibration characteristics of the transducer, the concentrator is usually shaped specifically to facilitate bonding by an axial motion along the wire to be bonded in an Al wire bonder. In addition to the effects of loading the wedge at the horn end, massive driver at the end of the transducer, and asymmetric clamping of the transducer, "mode conversions" occur and non-axial components are likely to be excited in the transducer. All vibration modes including axial, flexural and torsional, or their harmonics with frequency close to the operating frequency of the transducer are excited and they coupled together. Since the interferometer measures the absolute vibration amplitude normal to the transducer surface, the vibration displacement distributions measured are the resultant displacement of all the allowable modes being excited in the transducer.

Rael B. Morris et al. in 1991 used a p-version finite-element program to simulate the dynamic behavior of an ultrasonic transducer [7]. According to their simulation, high order non-axial modes were found near the transducer operating frequency, especially high-order flexural modes (the 13th flexural modes).

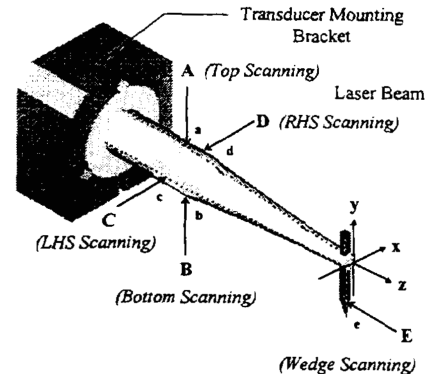

Fig. 2. 3-D diagram of the ultrasonic transducer.

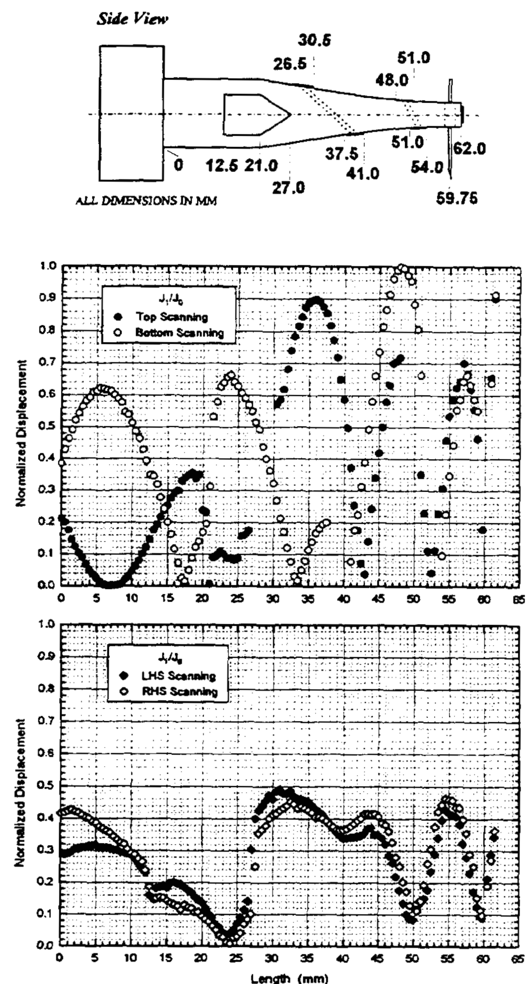

Fig. 3. Normalized vibration displacement distributions of the concentrator.

Authorized licensed use limited to: Hong Kong Polytechnic University. Downloaded on December 1, 2008 at 20:40 from IEEE Xplore. Restrictions apply.

C. Displacement Distributions of the Bonding Wedge

Since the wedge vibration is in orders of micron, in order to measure such a larger displacement without saturation of the interferometer, the driving voltage was reduced to 300 mV_{p-p} at the transducer terminal. The vibration displacement distribution of the wedge was measured, in steps of 0.25 mm, along the dotted line 'e' (wedge scanning), and the laser beam impinges on the wedge along direction 'E' (Fig. 2).

In Fig. 4, four anti-nodes and three nodes were observed along the length of the wedge, with two large-amplitude anti-nodes found at both ends. That is, the wedge vibrates in flexural mode. Magnification of displacement was also observed. The error of this experiment by comparing the result of $J_1(x)/J_0(x)$ to that of $J_2(x)/J_0(x)$ (not shown) is about 5%, and the measurement can be repeated to within about 10%.

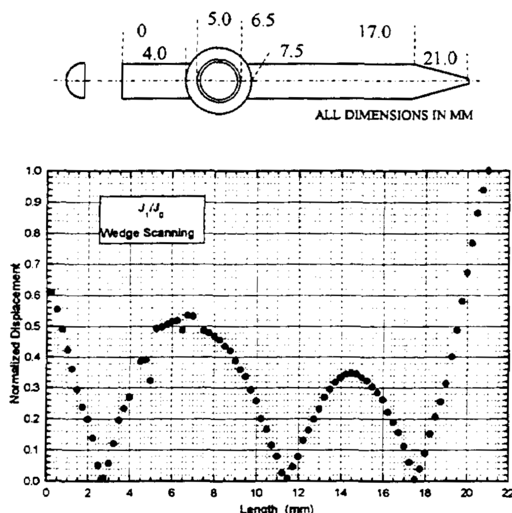

Fig. 4. Normalized vibration displacement distribution of the wedge.

III. Criteria For PZT Sensor Installation

Basically, there are three criteria for the choice of suitable location(s) on the transducer for PZT sensor installation. They are 1) the location should be capable of producing strong output signal from the sensor; 2) the location should be sensitive to the change of boundary conditions at the tip of the wedge; and 3) the location should be chosen such that the sensor would not be damaged during the bonding process.

IV. Bond Quality Monitoring Using Pzt Sensor

During bonding, the boundary conditions at the wedge tip change continuously. It is different depending on whether the tip is free, fixed, or damped in some way. A PZT sensor was attached on a suitable location on the transducer to sense these changes directly [8]. The bond quality monitoring system basically consists of a PZT sensor, a signal processor, a digital oscilloscope (HP 54522A), and a computer. The signal processor is comprised of a high input impedance pre-amplifier, a set of amplifiers, and a 2nd harmonic filter. The non-linear signal detected by the PZT sensor was processed by the signal processor and the ultrasonic signatures were recorded by the oscilloscope and saved in the computer. Pull tests and visual inspections were performed to check the bond quality. Good bond was defined as high pull strength and optimum wire deformation with small standard deviations.

Fig. 5 shows typical sensor signatures of a good bond. Only a small amplitude change and frequency shift is observed for the fundamental frequency (62.5 kHz), but a very characteristic amplitude change and frequency shift for the 2nd harmonic (125 kHz). When bonds are attempted without wire, the associated signatures are substantially different (Fig. 6) from those obtained with a good bond (Fig. 5). However, changes are still more significant for the 2nd harmonic. Poorly formed bonds are found to have signatures in between them or anomalous signatures depending on the degree of poorness, but again more significant changes are found in the 2nd harmonic. To illustrate how sensitive the system is, Fig. 7 shows the signatures of a poor bond due to inadequate calibration of the bonder. Low frequency tool bounce was observed in the 2nd harmonic during bonding, but not in the fundamental frequency.

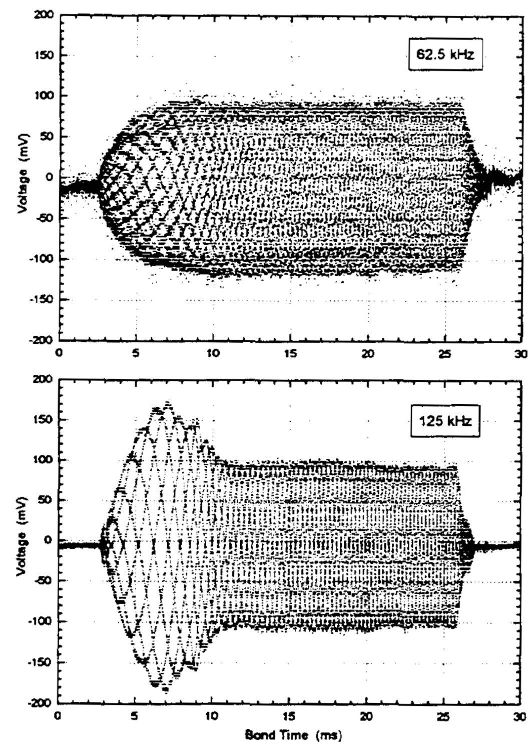

Fig. 5. Sensor signatures (62.5 kHz and 125 kHz) of a typical good bond.

Authorized licensed use limited to: Hong Kong Polytechnic University. Downloaded on December 1, 2008 at 20:40 from IEEE Xplore. Restrictions apply.

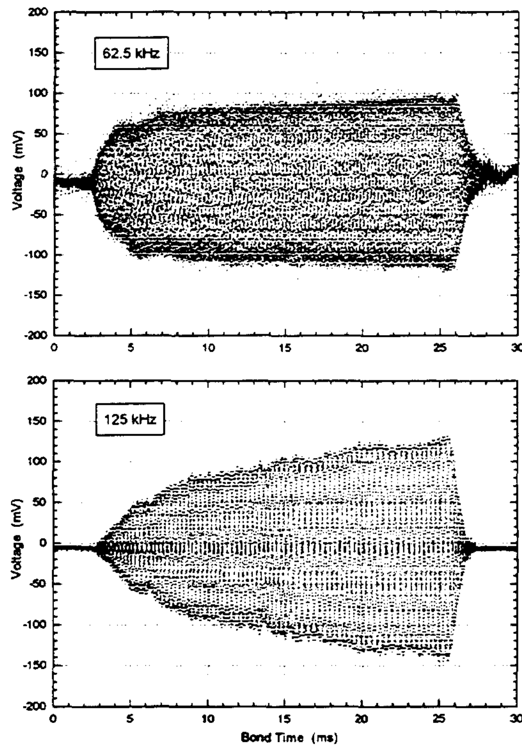

Fig. 6. Sensor signatures (62.5 kHz and 125 kHz) of a bond without wire.

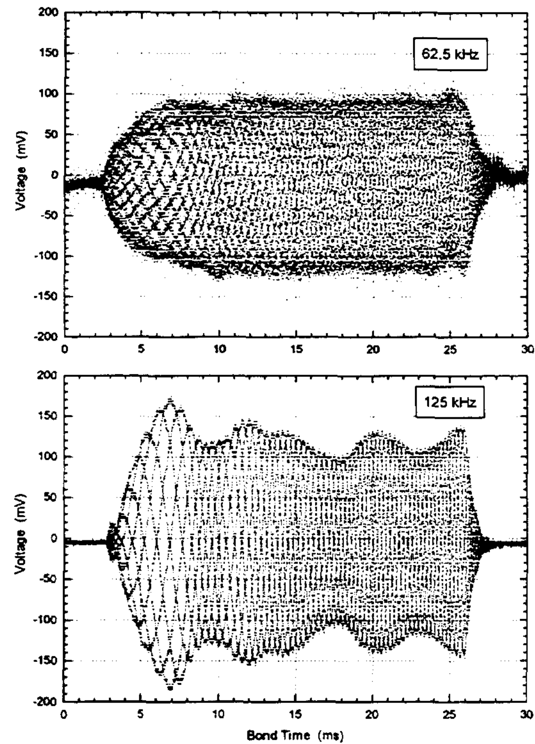

Fig.7. Sensor signatures (62.5 kHz and 125 kHz) of a poor bond due to inadequate calibration of the bonder.

VI. Conclusions

By attaching a PZT sensor on the transducer, the bond quality can be monitored by observing the 2nd harmonic of the ultrasonic signal. We believed that the most promising avenue for future development leading to an in-process quality control / monitoring technique for ultrasonic wire bonding lies in a multi-parameter approach based on modern data acquisition techniques. The findings in this work will be used to develop a multi-parameters real-time automatic process control system. Testing of the reliability of these signatures and their relations with bond quality in real bonding environment are in process.

Acknowledgment

Financial support from The Hong Kong Polytechnic University Teaching Company Scheme (TCS) is acknowledged.

References

[1] R. Rodwell and D. A. Worrall, "Quality Control in Ultrasonic Wire Bonding," *Hybrid Circuits*, No. 7, pp. 67-72, 1985.

[2] D. Royer and V. Kmetik, "Measurement of Pizeoelectric Constants using an Optical Heterodyne Interferometer," *Electronic Letters*, vol. 28, pp.1828-1830, 1992.

[3] D. Royer and E. Dieulesaint, "Optical Probing of the Mechanical Impulse Response of a Transducer," *Applied Physics Letter*, No. 49, pp. 1056-1058, 1986.

[4] B. Carlson, *Communication Systems - An Introduction to Signal and Noise in Electrical Communication*, 3rd ed., McGRAW-HILL International Editions, pp. 236-243, 1986.

[5] M. McBrearty, L. H. Kim and N. M. Bilgutay, "Analysis of Impedance Loading in Ultrasonic Transducer Systems," *IEEE Ultrasonic Symposium Proceedings*, vol. 1, pp. 497-502, 1988.

[6] L. G. Markulov and A. V. Kharitonov, "Theory and Analysis of Sectional Concentrators," *Soviet Physics - Acoustics*, 5, pp. 183-190, 1959.

[7] Rael B. Morris, Paolo Carnevali, and William T. Bandy, "Dynamics of an Ultrasonic Bonding Tool : A Case Study in P-version Finite-element Analysis," *The Journal of Acoustical Society of American*, 90(6), pp. 2919-2923, 1991.

[8] R. Pufall, "Automatic Process Control of Wire Bonding," *IEEE Proceedings*, pp. 159-162, 1993.

Authorized licensed use limited to: Hong Kong Polytechnic University. Downloaded on December 1, 2008 at 20:40 from IEEE Xplore. Restrictions apply.